

Nov. 1999

## **Sputter deposition of NiTi thin film exhibiting the SME at room temperatures**

Ken Ho, Greg P. Carman, & Peter Jardine

Mechanical & Aerospace Engineering, UCLA 38-137m Engineering IV, LA, CA 90095

### **ABSTRACT**

In this paper we will present a novel method for depositing NiTi thin film by DC sputtering that produces films with transformation temperatures very close to that of the target. The new process involves heating the target to temperatures over 400°C and does not require compositional modification of the 50/50atm% NiTi target. Results from tensile testing, XRD, TEM, and DSC are presented. Conclusion are, cold target produces films that were in the Austenite phase at room temperature while hot target produces films that were Martensite at room temperatures, confirming that compositional modification can be produced by varying the target temperature. Films that were produced by gradual heating of the target, produced a gradation of composition through the film thickness. These gradation produced films exhibiting the two-way SME. The simplicity of this new process should increase the use of NiTi films in microactuator devices.

### **1.0 BACKGROUND**

Thin film NiTi fabricated by sputtering offers a promising new material for solid state actuation in the MEMS field as well as new possibilities for medical devices. Since NiTi SMA shape memory alloys are heat actuated, improved performance can be achieved at microscales. Specifically, with a smaller mass and larger surface to volume ratio, heat transfer is substantially increased, power requirements are lowered, and large stresses and strains are achievable. These advantages make NiTi SMA a very promising actuation mechanism for microdevices. However, sputtering of NiTi thin film from a 50/50atm% NiTi target produces films with transformation temperatures different from the target due to loss of titanium during sputtering. This makes its use as an actuator questionable. Researchers have compensated for this, by placing Ti plates on the target to effectively alter the composition of the target, or to sputter off of a nonequalatomic NiTi target. A simpler approach is needed for the material to gain wider use in the MEMS community.

NiTi is a shape memory alloy (SMA) that is capable of recovering strains on the order of 10%. This effect, which is termed the shape memory effect (SME), occurs when the material undergoes a phase transformation from the low temperature martensitic phase to the high temperature austenitic phase. In the martensitic phase the material is deformed by preferential alignment of twins. Unlike permanent deformations associated with dislocations, deformation due to twinning is fully recoverable when heated to the austenite phase. The SME is a one way effect, that is the material recovers its original shape after heating to the austenite phase but does not revert back to its deformed state when cooled. In order to achieve cyclic actuation, a biasing force such as a spring is necessary to deform the material when in the martensitic phase. Implementing a bias force on thin film structures present significant manufacturing obstacles, an additional challenge for using thin film NiTi as a MEMS actuator.

The first work to incorporate thin film NiTi with a micromachining process was done by Walker et al. in 1990 [1]. They used a wet chemical etchant ( $\text{HF} + \text{HNO}_3 + \text{H}_2\text{O}$ ) to pattern a free standing serpentine NiTi spring. The structures were curled when released and uncurled when heated, they attributed this to the shape memory effect. However, their films were amorphous as deposited. In 1990 Bush and Johnson at the TiNi Alloy Company showed the first definitive evidence of SME in NiTi films [2]. Using a single target (50/50atm% NiTi), with a DC magnetron sputtering system they presputtered

for 3 hours. Sputtering of the film was performed with a  $P_{Ar} = 0.75\text{mTorr}$ ,  $V=450\text{V}$ ,  $I=0.5\text{A}$  and a target substrate distance of 2.25 inches. The as deposited film was shown by XRD to be amorphous and after vacuum annealing at  $550^\circ\text{C}$  for 30 minutes exhibited the SME although transformation temperatures were  $100^\circ\text{C}$  lower than the target material.

NiTi films with transformation temperatures above room temperature are difficult to achieve. Sputtering directly from a 50/50 atm % NiTi target results in films with dramatically lowered transformation temperatures, prohibiting its use as an actuator [2]. This is caused by the fact that NiTi alloys are strongly dependent on composition, annealing temperatures, aging time, and sputtering parameters [3-5]. Of these alloy composition is the most critical. Figure 1 shows the dependence of transformation temperature on Ni-Ti stoichiometry, a shift of as little as 1atm% can alter transformation temperatures by  $100^\circ\text{C}$ . Shifts typically occur during sputtering because titanium reacts fairly easily. Titanium is typically used to getter materials, and are often used in vacuum systems to pull down a vacuum by reacting with the gases and condensing. Because of this, during sputtering the film typically shows a slight deficiency in titanium from the target material. Miyazaki et al. [6] compensated for the titanium loss by placing titanium plates on top of the alloy target; Heuer et al. [7] similarly compensated with titanium foils, and A. Gyobu et al. [8] also recently sputtered from a 50/50 NiTi target using titanium compensation. The other method of compensating for the titanium loss is to use a multigun cosputtering system. For example, Kruevitch et al. used a dc magnetron system to sputter from individually powered Ni, Ti, and Cu targets [9].

A further complication is that the NiTi phase is very narrow at low temperatures as indicated by its phase diagram in figure 2. This indicates that slight shifts in stoichiometry of the material easily causes precipitate formation complicating the metallurgical factors in relating a heat treatment to the transformation temperatures. Therefore, it would be advantageous to develop a simple approach that could produce deposited film with composition similar to the target.

In addition to difficulties in depositing, films typically exhibit the one way shape memory effect only. To achieve the two-way effect a biasing force is required to reshape the NiTi when cooled. Kuribayashi introduced this biasing force by tailoring precipitates in his films such that there were compressive and tensile stresses on opposite sides of his film [10]. The film curled when in the martensitic phase and when heated to the austenite phase flattened because the higher modulus overcomes the residual stresses. This process requires complicated heat treatments and the stability of these precipitates after numerous thermal cycles are not known. For macroscopic systems individuals are proposing to combine superelastic elements with shape memory elements to achieve the two-way effect. Therefore it might be advantageous to develop an approach to produce compositionally graded thin films for achieving the two-way effect.

Thin film TiNi actuators are well suited for MEMS devices because of their large work energy densities. However, the difficulties associated with depositing this material has limited its access by the MEMS community. To address this issue, researchers focused on deposition, heat treatments, and thermomechanical characterization [11-15] of the film and only a handful of researchers developed actual microdevices. The TiNi Alloy Co. has a working microvalve it markets, which closes using a bias mass and opens when the thin film NiTi ligaments are heated. Kruevitch et al. fabricated a  $900\mu\text{m}$  long,  $380\mu\text{m}$  wide, and  $200\mu\text{m}$  tall microgripper from  $5\mu\text{m}$  thick NiTi-Cu film, as well as a functioning microvalve [9]. Benard et al. fabricated a micropump from NiTi film using two designs: polyimide as the biased actuator in one and a complementary NiTi actuator in the other [16]. Kuribayashi et al. [17] used TiNi films to actuate a microrobotic manipulator

In this research we developed an approach to deposit, a 50/50atm% NiTi film without compositional modification. Films with transformation temperatures similar to the target can be produced by heating the target to temperatures greater than  $400^\circ\text{C}$ . An unheated target produced austenitic films from the same target. When the target is gradually heated compositional variation through the thickness can be achieved producing the two-way SME. Therefore the proposed approach can be used to fabricate useful MEMS actuators exhibiting the two-way effect.

## 2.0 Sputtering Process

A sputtering system was fabricated at UCLA to deposit NiTi. The goal was to achieve an ultra clean, contamination free system. A picture and schematic of the system is shown in figure 3. The system is UHV (ultra high vacuum) compatible with a loadlock to decrease pump down time as well as eliminate contamination. An RGA (residual gas analyzer) is present to monitor contamination levels, particularly oxygen and water pressures, prior to sputtering. An argon scrubber is used to further clean the 99.999% purity argon gas. Sputtering is done with a 3" DC magnetron gun from US Thin Film Products Inc. An in-situ heater with rotation capability is used to crystallize the films.

Films were deposited using the following parameters: base pressures  $<5 \times 10^{-8}$  Torr,  $P_{Ar} = 2.0$  mTorr, target substrate distance = 3cm, and power = 300W. The films were crystallized by heating the substrate to 500°C and holding it at this temperature for 6 minutes. In this study we will focus on two fabrication processes: the first process is film sputtered off of a cold target  $<100^\circ\text{C}$  (C samples), the second process is film sputtered off of a hot target  $>400^\circ\text{C}$  (H samples). The temperature profile of the hot target as a function of sputtering time is presented in table 1.

TABLE I

Time (min)	Temp ( $^\circ\text{C}$ )
0	30
5	310
10	540
15	650

The films deposited by the two methods were measured using a profilometer and found to be approximately  $3\mu\text{m}$  thick. In observing the film while attached to the substrate, the C samples were shiny after deposition and crystallization, indicating a high modulus austenite phase. H samples however were cloudy when cooled and shiny when heated up. Sputtered films have tensile residual stresses such that when the NiTi film is in the martensitic phase it accommodates these stresses by twinning, thus its surface is more textured and therefore cloudy. This suggests and tests results confirm that at room temperature the C samples are austenite and the H samples are martensite. Substrates used in depositing the NiTi films included 4 inch silicon wafers, glass slides, nitride wafers and oxide wafers. It was found that the H sample and C sample films showed respectively similar texture regardless of substrates. Therefore results presented in this paper are primarily associated with glass substrates.

## 3.0 Discussion

Currently it is difficult to sputter NiTi films with transformation temperatures above  $25^\circ\text{C}$  from a single unmodified 50/50 atm % NiTi target. However, we found that by increasing the target temperature, films with transformation temperatures above  $25^\circ\text{C}$  from an unmodified 50/50 atm% NiTi target could be obtained. We also discovered that by controlling the target temperature films exhibiting the two-way SME could be produced. A discussion of these results follow.

Heating the target also radiatively heats up the substrate. This was thought to be a possible mechanism that might be responsible for stabilizing the composition during sputtering. To address this issue, the substrate was heated to four different temperatures while the target was kept cold. Films were sputtered with the substrate heated to  $200^\circ\text{C}$ ,  $300^\circ\text{C}$ ,  $500^\circ\text{C}$ , and  $600^\circ\text{C}$ . XRD presented later will show that the films were austenitic and not martensitic at room temperatures. Thus, the process of heating the target during sputtering is not equivalent to conventional substrate heating.

Cleanliness of the target was another issue. Heating the target degasses any contaminants present on the surface. To evaluate if this contributed to the difference in transformation temperatures between the H samples and C samples, presputtering was performed. The cold target was presputtered

for two hours, which would be sufficient to remove any surface contaminants and achieve uniformity in the sputtering rates. However, presputtering did not influence the material properties, therefore we concluded that presputtering had negligible effect in altering the transformation temperatures of the C samples. In contrast, the H samples were presputtered for only 10-minutes and subsequent runs were not presputtered. This is possible because the loadlock keeps the target in vacuum. Therefore, presputtering and target cleanliness does not contribute to altering the transformation temperatures of the H samples.

One possible explanation of why heating the target produces martensitic films may be that the binding energy is lowered. The lowered binding energy would result in an increased sputtering yield as given by the following equation [18]:

$$S \propto \frac{K}{U} \left( \frac{M_i}{M_t} \right)$$

Where S is the sputtering yield, K is the kinetic energy of the incident ion, U is the binding energy, and  $M_t$ ,  $M_i$  are the mass of the target atom and incident ion respectively. The increased sputtering yield would be similar to increasing the sputtering power, which we have observed to correlate similarly, but to a lesser degree than target temperature, on altering the transformation temperature of the deposited films. Therefore, increasing sputter yield maybe one possible explanation but this topic is still being investigated.

The H sample films also exhibit a two-way shape-memory effect. The resulting two-way effect is intrinsic in the processing step and does not require further heat treatments. Figure 4 shows the film at three stages: 25°C, 150°C, and back to 25°C. Without external biasing the film, the film is initially flat, curled when heated and uncurled when cooled back to room temperature. We attribute this to the fact that the film is nonuniform across its thickness with a slight gradation in composition. We hypothesize that the lower part of the film is austenite and the top part is martensite, possibly a superelastic system combined with a shape memory system (figure 5a). This is because the target temperature increases during deposition, so that the initial deposition occurs with a cold target resulting in the bottom portion of the film being austenitic. Thus when the film is heated, the upper martensite transforms to austenite, causing the film to curl. When cooled the stresses induced by the thin austenite layer are sufficient to twin the martensite and return the film to the flat configuration. The two way effect has also been used to fabricate a MEMS bubble actuator recently.

At this point control of the target temperature is not precise, but if accurate control is possible a tailored 2-D austenite-martensite bimorph can be fabricated (figure 5b). The proportion of austenite to martensite can be tailored resulting in a predefined force-displacement response. With this process NiTi film can be fabricated with the two-way effect without complicated heat treatments that might be incompatible with MEMS processing. Hopefully, this will increase the usefulness of NiTi films for MEMS devices.

Our novel sputtering process is less complicated than a multigun cosputtering system. Using a multigun system not only requires expensive equipment, but a calibration of each gun to the proper sputtering. Generally this would mean an expensive and complicated feed back system with deposition rate monitoring, or calibration of each gun separately then recalibrating as deposition conditions drift with time. The process of using titanium plates or foils has the problem of repeatability as the plates wear down. To date, the process we introduce is inexpensive and produces repeatable film compositions run after run. We have made over 10 samples from a single target with consistent results.

## 4.0 Characterization Studies

### 4.1 Materials Testing

XRD (x-ray diffraction) was performed on the samples to determine the NiTi film's crystalline phase. The C sample displayed XRD patterns at 25°C indicative of an austenite phase (figure 6). XRD on the H samples immediately after deposition indicated that the material was not completely martensitic,

but a mixture of martensite and austenite (figure 7a). When cycled down to -100°C then back to 25°C, XRD pattern indicated that the H sample film was now completely martensitic (figure 7b). The film therefore exhibits a hysteresis seen in bulk NiTi due to the growth and shrinkage of martensitic regions within austenite. The difference however, is that the austenite and martensite in our film is believed to be gradated through the thickness rather than randomly distributed phases.

To verify that heating the target was not indirectly causing substrate heating, samples were deposited on a hot substrate while keeping the target cold. XRD of these samples are given in figure 8. The films were deposited on a hot substrate at four different temperatures 200°C, 300°C, 500°C, and 600°C and subsequently annealed at 500°C for 6 minutes after deposition to ensure that the films were crystallized. XRD confirm that all films are austenitic at room temperatures. Cycling the temperature down to -50°C and back to 25°C did not alter the XRD patterns. An extra peak in the XRD at  $2\theta = 37.7^\circ$  begins appearing at higher substrate temperatures and grows with increasing substrate temperatures (compare figures 9a-9d). This peak corresponds to a  $\text{Ni}_4\text{Ti}_3$  precipitate peak. Substrate heating did not produce martensitic films as did target heating but rather induces precipitate growth.

To confirm the presence of the precipitates TEM studies were done on the 600°C substrate heated sample. The sample was initially 3 $\mu\text{m}$  thick and was thinned down using an ion mill. Figure 9 shows the presence of intergranular precipitates verifying the XRD results. These will influence the shape memory response and produce a more brittle film. The precipitates were measured to be 20nm in size. The NiTi grains vary from 0.1 $\mu\text{m}$  to 1 $\mu\text{m}$  in size. Atomic force microscope results of the H film showed a comparable grain size.

Transformation temperatures for the film were measured first with a DSC. DSC results for the H sample given in figure 10. Data shows a peak that is short and broad in width during the exothermic M to A transformation and the endothermic A to M transformation. The area under these peaks correspond to the latent heat of transformation, such that a short and broad peak would indicate that martensite is growing and shrinking in different regions at different  $M_s$  and  $A_s$  temperatures. This would indicate that the H sample films are not uniform across the thickness, but rather is transforming over a broader temperature region. We do admit that, nonuniformity across the film area would also give similar results. However, because of the observed two way effect, we believe that gradation through the thickness is the attributing factor. Figure 11 is DSC of a rolled film showing transformation points that are more distinct, typical of a film with more uniform phases. Transformation temperature results from DSC of the C and H samples compared to the Tf given by the manufacturer of the target material is given in table II. The Tf of the H sample is comparable to that of the target indicating that there was very little compositional deviation from the target material.

**TABLE II DSC Results**

Sample	As	Af	Ms	Mf
Target (from manufacturer)	95°C	110°C	68°C	55°C
H sample (Hot target)	80°C	105°C	60°C	20°C
C sample (Cold target)	-7°C	22°C	-100°C	-150°C

## 4.2 Mechanical Testing

The mechanical properties of the H sample films were characterized in an MTS microforce testframe. Sample films 3.5 $\mu\text{m}$  thick 1.5cm in length and 4.5mm in width were prepared. The stress strain curves of an H sample film at two temperatures are shown in figure 12a. During the 100°C run the film was heated with a heat gun and temperature was measured with a thermocouple near the film. Slight temperature fluctuations produced by the heat gun accounted for the jaggedness of the curve. Recently a thermal chamber for the system was acquired and more accurate characterization is underway. The film produces a recovery strain of 5%, and failure does not occur until strains greater than 10% are applied. The maximum recovery force defined by the load when the film is heated to the austenite phase is 150ksi. Tensile tests were also performed on a strip of target material 1.5cm in length x 2.5mm in width and

0.16mm in thickness to give a reference (figure12b). Due to the increase in sample size, stress was limited to below 45ksi on the target sample. The two material (i.e. the film and target) showed comparable yield strengths (i.e. 40 ksi). Films produced by Miyazaki by using titanium plates as compensation also have comparable mechanical characteristics as the H sample films (figure13). For example both films begin showing increase stiffness after 4% strain indicating dislocation pile-up maybe occurring.

## 5.0 Membrane actuator for active flow control

Currently our research group is working on developing a microscale actuator for active flow control. Active Flow Control (AFC) represents an advanced concept for reducing drag, controlling flow separation, improving flight control effectiveness, and manipulation of wake vortex interactions in aircraft systems. This concept has been around for the last 30 years. The obstacle to its successful implementation has been a lack of a compact rugged sensor-actuator technology. In recent years the combined evolution of MEMS (microelectromechanical systems) technology and active materials has produced advancements that can make AFC very close to being a reality [19].

Our concept for microscale actuated flow control is to fabricate a NiTi bubble membrane using standard lithographic approaches that will produce out-of plane actuation (figure 14). When resistively heated the membrane actuator extends into the flow field and when cooled it flattens out. This actuator thus exhibits a two-way effect. Recently Favelukis et al [22]. demonstrated analytically that frequency response rates can exceed 300Hz. The actual device fabricated was 3mm in diameter producing 500 $\mu$ m of vertical displacement when heated (figure 15). Although the actuator was designed for possible use in active flow control, the simplicity of the device will allow it to be adapted as an actuation scheme in many other devices, such as micropumps, microvalves, and micro switches.

## 6.0 CONCLUSION

Sputter deposition of NiTi films exhibiting the SME above 25°C is difficult. This is because of the sensitivity of the shape memory characteristics to composition and the relative ease with which titanium is lost during sputtering. As a consequence, sputter deposition from a single 50/50 atm% NiTi target typically requires compensation with titanium plates. A multigun cosputtering system could also be used but this process is more expensive and complicated. In this paper we have shown that by heating the target to over 400°C during deposition, films exhibiting the SME above 25°C can be produced from an unmodified 50/50 atm% NiTi target.

A dedicated UHV sputtering system was built and NiTi films with  $A_s >$  room temperature was deposited. Materials characterization indicate that certain films have a gradation in stoichiometry through its thickness. This was attributed to the variation of target temperatures during sputtering. The bottom of the film being austenitic when the target was initially cold and martensitic at the top when the target increased in temperature. As a result of this gradation the two way effect was observed in free standing films and a bubble actuator.

Mechanical testing using an MTS Tytron microforce testframe showed that the films had recovery strains of 5% and failed at strains exceeding 10%. The stress-strain behavior was comparable to the bulk NiTi target and films produced by Miyazaki et.al. using titanium plates as compensation.

We have shown that the process of sputtering with the target hot can produce NiTi films with the SME at room temperatures. The process can be used to tailor a 2-D austenite-martensite bimorph structure that would give the two way SME without complicated heat treatments. The simplicity of the process will allow the MEMS community more access to NiTi films for microactuation. We have fabricated a 3mm diameter NiTi membrane actuator capable of 500 $\mu$ m of vertical deflection for use in microscale actuated flow control. The same membrane actuator can be used in microdevices such as micropumps, and microvalves.

### **ACKNOWLEDGEMENTS**

The authors of this paper gratefully acknowledge the support from the Air Force Office of Scientific Research (AFOSR) under contract number F49620-98-1-0058 contract monitor Brian Sanders. We also would like to acknowledge an equipment grant to develop a ultra-high-vacuum sputtering for TiNi thin film by the National Science Foundation CMS-9622283

## REFERENCES

1. J.A. Walker, K.J. Gabriel, and M. Mehregany, Sens. Actuators, vols. A21-A23, p. 243, 1990.
2. J.D. Busch, A.D. Johnson, et. al., "Shape-memory properties in Ni-Ti sputtered-deposited film", J. Appl. Phys., Vol.68, p.6224, 1990.
3. S. Miyazaki, et.al., "Effect of heat treatment on deformation behavior associated with R-phase and martensitic transformations in Ti-Ni thin films", Trans. Mat. Res. Soc. Jpn., Vol. 18B, pp1041, 1994.
4. A. Ishida, M.Sato, A. takei and S. Miyazaki, "Effect of heat treatment on shape memory behavior of Ti-rich Ti-Ni thin films", Materials Transactions, JIM, vol. 36, p.1349, 1995.
5. A. Peter Jardine, "Deposition parameters for sputter-deposited thin film TiNi", Mat Res. Soc. Symp. Proc., Vol 360, p. 293, 1995.
6. S. Miyazaki and K. Nomura, "Development of perfect shape memory effect in sputter-deposited Ti-Ni thin films", Proceedings IEEE Microelectro Mechanical Sys., p.176, 1994.
7. R.H. Wolf and A.H. Heuer, "TiNi (Shape Memory) Films on Silicon for MEMS Applications". J. of Microelectromechanical Sys., vol.4, no.4, p.206, 1995.
8. A. Gyobu, Y. Kawamura, H. Horikawa, and T. Saburi, "Martensitic transformations in sputter-deposited shape memory Ti-Ni films", Mat. Trans. JIM, vol. 37, no.1-6, p.697, 1996.
9. P. Krulevitch, A.P. Lee, P.B. Ramsey, et.al., "Thin film shape memory alloy microactuators", J. of Microelectromechanical Sys., vol.5, no.4, 1996.
10. K. Kuribayashi, T. Taniguchi, M. Yositate, and S. Ogawa, "Micron sized arm using reversible TiNi alloy tin film actuators". Mat. Res. Soc. Symp. Proc., vol.276, p.167, 1992.
11. J.D. Busch, M.H. Berkson, and A.D. Johnson, Phase transformations in sputtered NiTi film: effects of heat treatment and precipitates. Mat. Res. Soc. Symp. Proc., vol.230, p.91, 1992.
12. D.S. Grummon and T.J. Pence, "Thermotractive titanium-nickel thin films for microelectromechanical systems and active composites", Mat. Res. Soc. Symp. Proc., Vol.459,p.331, 1997.
13. Q. Su, S.Z. Hua and M. Wuttig, "Martensitic transformation in NiTi films", J. of Alloys and Compounds, vol.211, p.460, 1994.
14. S. Miyazaki, et.al., "Shape memory characteristics of sputtere-deposited Ti-Ni base thin films", SPIE, vol.2441, p.156, 1995.
15. A. Ishida, A. Takei, M. Sato and S. Miyazaki, "Shape memory behavior of Ti-Ni thin films annealed at various temperatures", Mat. Res. Soc. Symp. Proc., vol.360, p.381, 1995.
16. W.L. Benard, H. Kahn, A.H. Heuer and M.A. Huff, "Thin film shape memory alloy actuated micropumps", J. of Microelectromechanical Systems, vol.7, no.2, 1998.
17. K. Kuribayashi, S. Shimizu, T. Nishinohara and T. Taniguchi, "Trial fabrication of micron sized arm using reversible TiNi alloy thin film actuators", Proceedings International Conf. On Intel. Robots and



Sys., Yokohama, Japan, p.1697, 1993.

18. R.F. Bunshah, Handbook of Deposition Technologies for Films and Coatings. Noyes Publications, Park Ridge, NJ, 2<sup>nd</sup> Edition, 1994.
19. C.M. Ho and Y. Tai , "Mems:Science and Technology," Application of Microfabrication to Fluid Mechanics, FED V. 197, ASME 1994, pp. 39-49, 1994.
20. T.W. Duerig, K.N. Melton, D. Stockel and C.M. Wayman, Engineering Aspects of Shape Memory Alloys, 1990.
21. T.B. Massalski, Binary Phase Diagrams, American Society for Metals, Metals Park, OH, 1986.
22. J.E. Favelukis et al., "An experimentally validated thermal model of thin film NiTi" SPIE (unpublished).

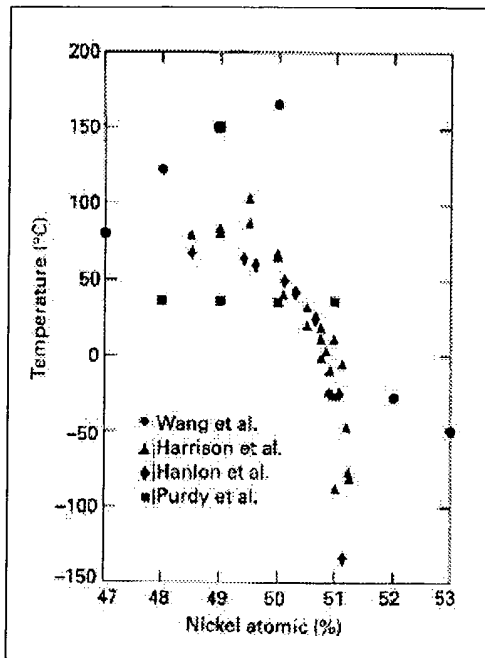


Figure 1. Compositional sensitivity of NiTi transformation temperature[20]

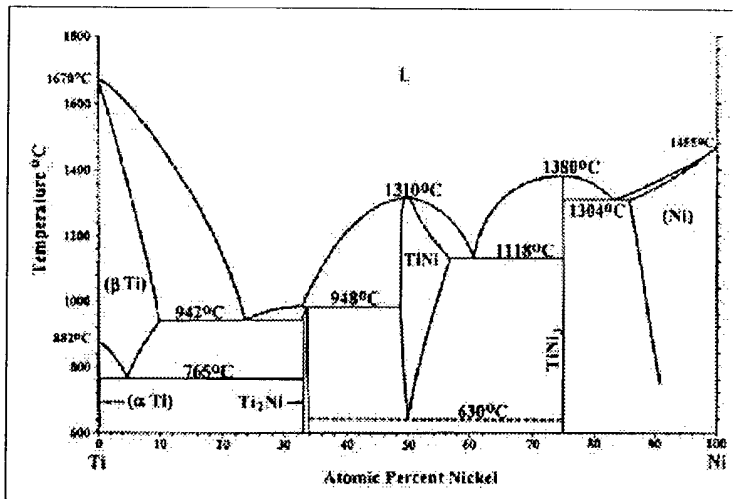


Figure 2. NiTi phase diagram [21].

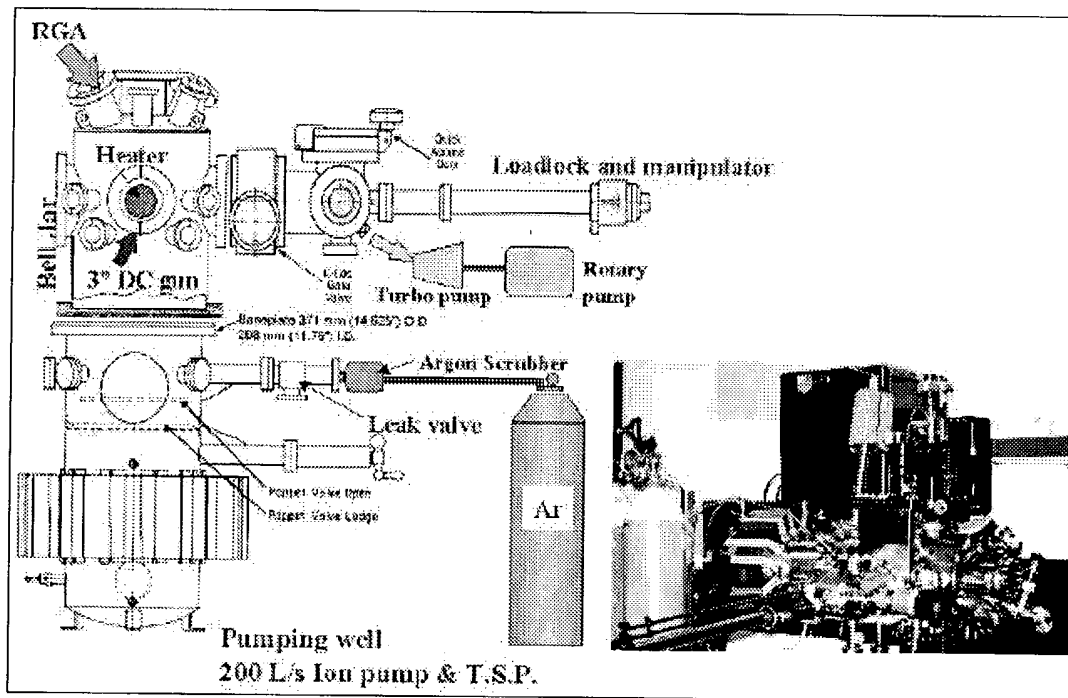


Figure 3. Schematic and picture of UHV sputtering system for thin film NiTi.

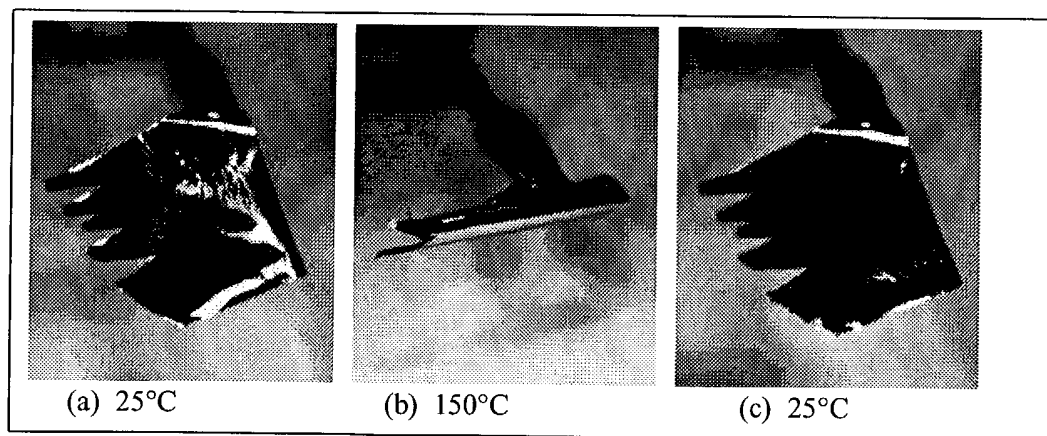


Figure 4. Free standing NiTi film exhibiting the two way shape memory effect.

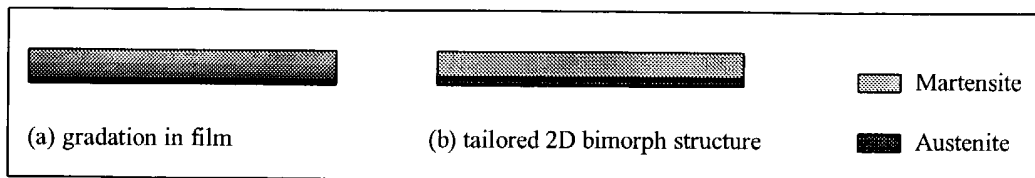


Figure 5. a) Gradation of film due to gradual heating of the target accounting for the two-way SME. b) More precise tailoring for a 2-D bimorph structure is possible.

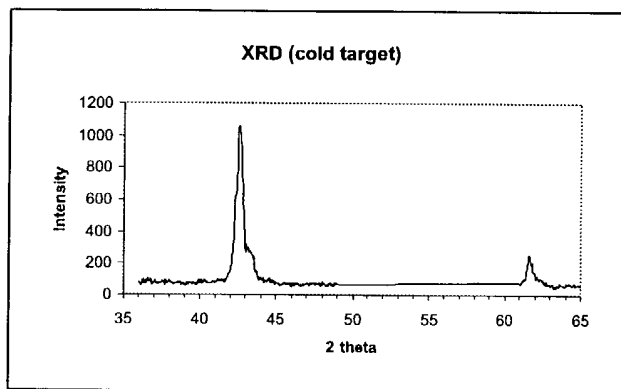


Figure 6. XRD of film sputtered from a cold target indicating an austenite phase at 25°C.

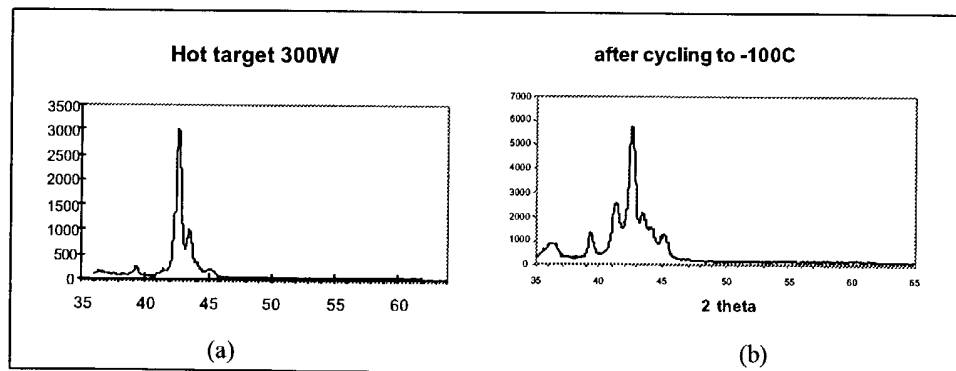


Figure 7. a) XRD of film sputtered from a hot target. b) after cycling to  $-100^{\circ}\text{C}$  then back to  $25^{\circ}\text{C}$  film is completely martensitic.

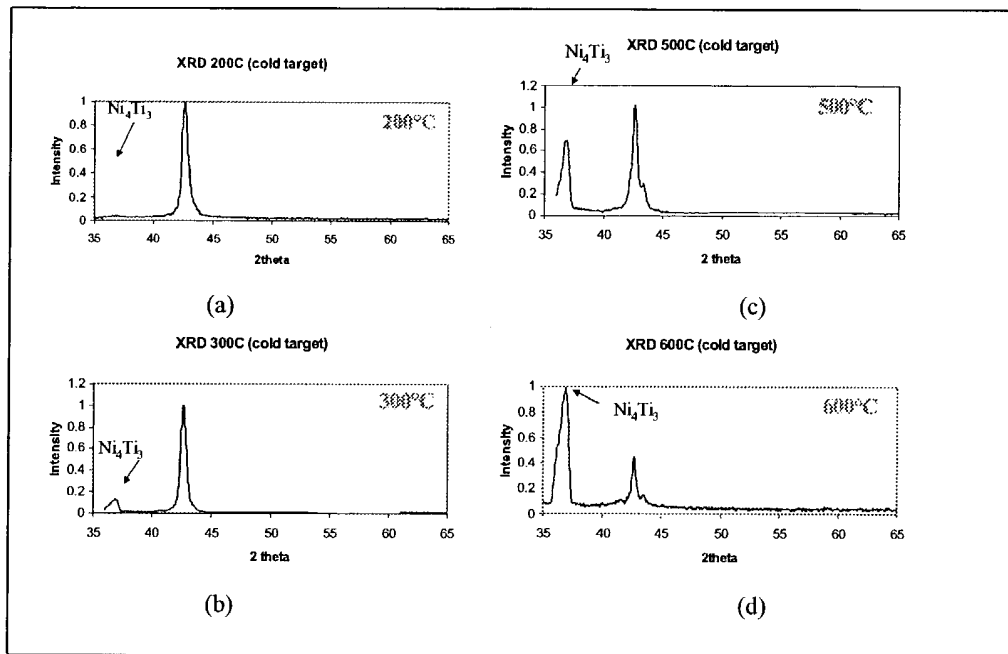


Figure 8. XRD of films sputtered with a cold target and substrate heating. The extra diffraction peak at  $2\theta = 27.6^\circ$  grows with increasing substrate temperature and corresponds to a  $\text{Ni}_4\text{Ti}_3$  precipitate.

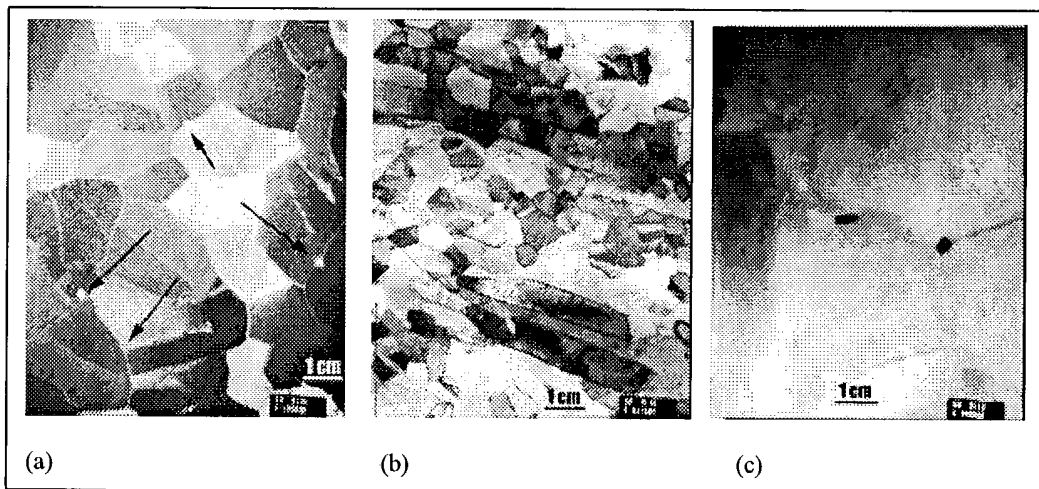


Figure 9 a) 105,000X magnification, dark field image showing presence of precipitates b) 37,500X magnification, bright field image showing variation in grain sizes of 0.1-1  $\mu\text{m}$ . c) 380,000X magnification, bright field image showing 20nm size precipitate.

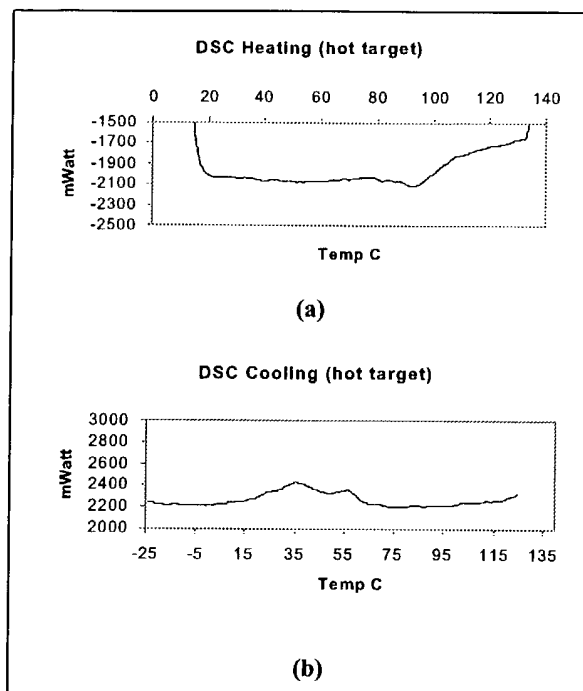


Figure 10 DSC of film deposited from a hot target.

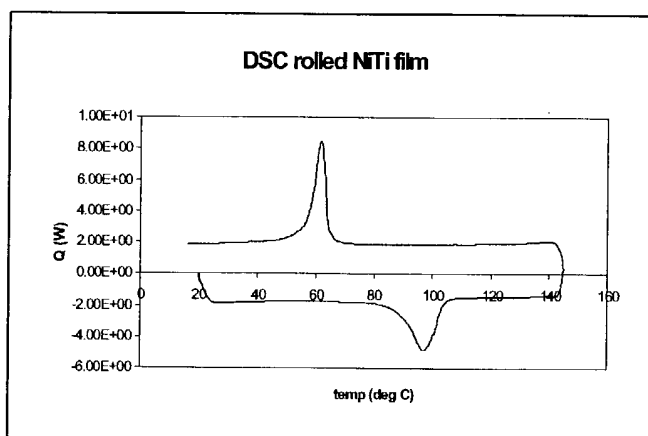


Figure 11 DSC of a typical rolled film.

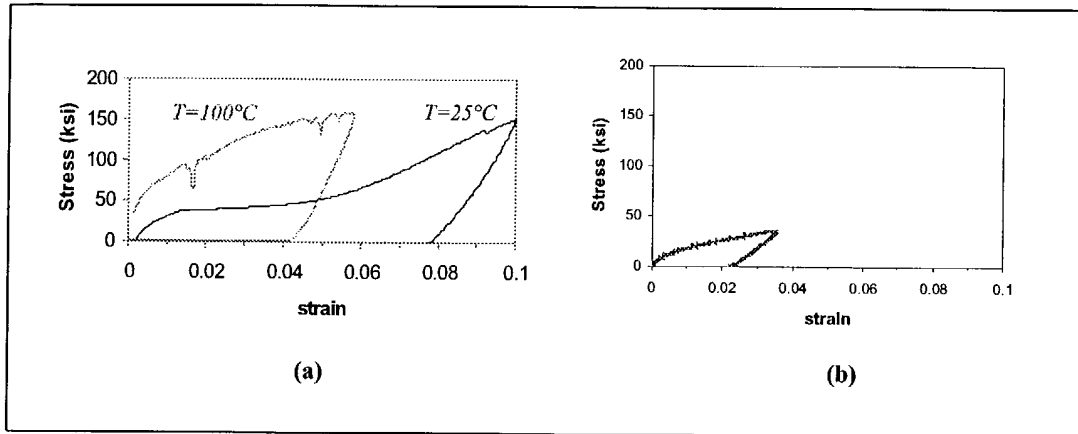


Figure 12 a) Stress-strain curve of sputtered film at  $100^{\circ}\text{C}$  and  $25^{\circ}\text{C}$ . b) Stress-strain curve of a strip of target material.

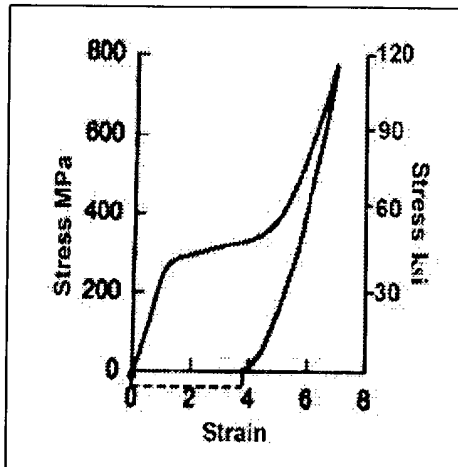
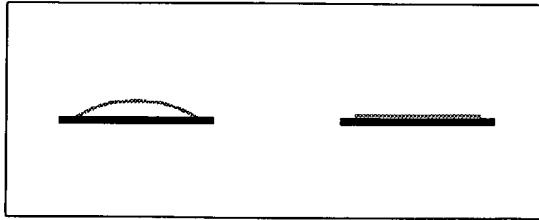
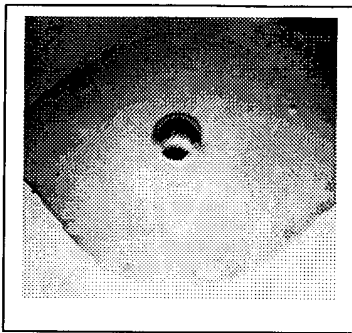


Figure 13 Stress strain curve results of sputtered films by other Authors. (Ref. Miyazaki)



**Figure 14** Concept of actuator for active flow control. a) heated shape b) cold shape



**Figure 15** Fabricated NiTi membrane actuator in the heated shape.



Cambridge Scientific Abstracts

**MicroElectroMechanical Systems (MEMS)**  
Hot Topics Series**The fabrication of thin film NiTi shape memory alloy mems actuator for MEMS application**

Gill, John J; Ho, Ken; Carman, Gregory P

IN: Adaptive structures and material systems - 1999; Proceedings of the Symposium, 1998 ASME International Mechanical Engineering Congress and Exposition, Nashville, TN, Nov. 14-19, 1999 (A00-42276 11-31), New York, American Society of Mechanical Engineers (ASME Aerospace Div./Materials Div., AD-Vol. 59/MD-Vol. 87), 1999, p. 125-131

A novel two-way thin film NiTi shape memory alloy actuator is presented. Thin film shape memory alloy is sputter-deposited onto a silicon wafer in an ultra high vacuum system. Transformation temperatures of the deposited NiTi film are measured by residual stress measurement at temperatures from 25 C to 120 C. Test results show that the  $M_f$  (the Martensite Finish Temperature) is around 60 C and  $A_f$  (the Austenite Finish Temperature) is around 110 C. A free standing NiTi membrane (10 mm x 10 mm and 3  $\mu$ m thick) is fabricated using MEMS technology. We found that a mixture of HF, HNO<sub>3</sub>, and DI (deionized) water with thick photo resist mask works best for the fabrication process. The membrane is hot-shaped in different shapes such as dome shape, pyramidal shape, and cylindrical shape. Results indicate that when the temperature of the NiTi film exceeds  $A_f$ , the NiTi membrane transforms into the trained hot-shape. When the temperature cools down to room temperature, the membrane returns to the initial flat shape. (Author)

---

[| Next Paper](#) | [Previous Paper](#) | [List of Key Citations](#) |